

§29. Observation of Ablation Clouds of Lithium Doped Tracer-encapsulated Solid Pellets with a Stereoscopic Fast Framing Camera System

Shoji, M., Tamura, N.,
de la Cal, E., van Milligen, B., de Pablos, J., Hidalgo, C.
(EURATOM-CIEMAT)

A fast framing CMOS camera (Photoron APX-RS) introduced from CIEMAT has been applied for the measurement of the trajectory and ablation process of Lithium doped tracer-encapsulated solid pellets (TESPEL) and for impurity transport analysis in LHD plasmas.¹⁾ In the 15th experimental campaign, the trajectories of the TESPEL were measured with a stereoscopic fast framing camera system. It consists of two optical lenses, two image fibers, a stereo-optics, two filter wheels (Optec IFW) and the fast framing camera. An interference filter can be selected from eight ones (H_{α} , CII, CIII, Brems., LiI, LiII, and two ND filters) by rotating the wheels which are controlled from the LHD control room via mediaconverters and a RS-232C serial device server (Moxa NPort 5210). An image intensifier was not necessary in the measurements because of high intensity of the ablation clouds of the TESPEL, which contributes to taking highly spatially resolved images.

The stereoscopic camera system was installed in an outer port (3-O). The optical lenses were mounted at an upper left side and a right side viewport from the position of the TESPEL injection port for getting three-dimensional trajectories of the pellets with a good spatial resolution.

Figure 1 (a), (b) and (c) show three typical stereoscopic images of ablation clouds of the TESPEL (Li

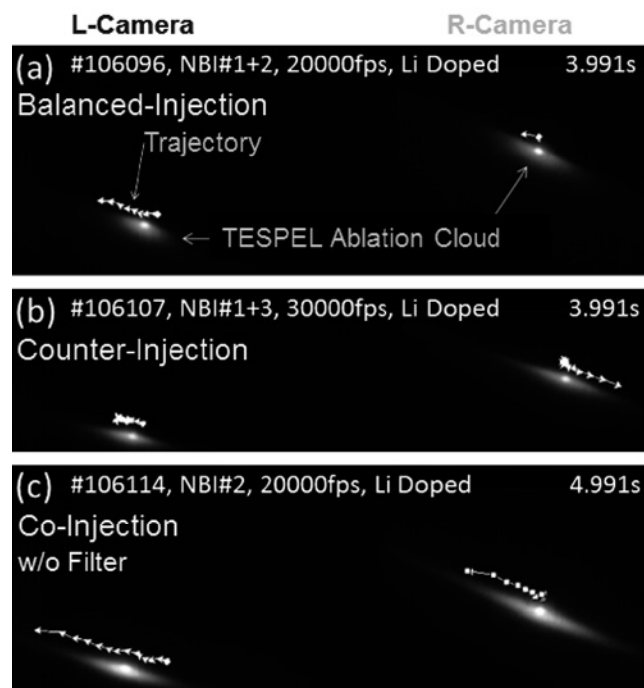


Fig. 1 Stereoscopic images of the ablation clouds of Li doped pellets (TESPEL) in (a) balanced-, (b) counter- and (c) co-NBI heating cases for $R_{ax}=3.60m$.

doped) which were taken in a balanced-, counter- and co-NBI heating cases for $R_{ax}=3.60m$ without interference filters, respectively. Left and right figures are the images of the ablation clouds observed from the upper left and the right side view ports with frame rates (20000 or 30000fps), respectively. Chains of the white arrows in the figures represent the observed trajectories of the central bright position of the ablation clouds. The trajectories of the ablation clouds on the stereoscopic images strongly depend on the toroidal direction of the NBI heating.

Image analysis of the ablation clouds provides three-dimensional trajectories of the ablation cloud. Thus, a pinhole camera model, which was used for the analysis of the trajectories of fueling pellets in the LHD, was applied.²⁾ In advance, a spatial calibration was carried out using a flat board on which grid markers are printed. By moving the board from front to back, a database of the spatial correlation between the three-dimensional positions of the markers and the pixel positions on the stereoscopic image (totally 564 points) was constructed. Figure 2 (a) and (b) show the three-dimensional trajectories of the ablation clouds in the three different NBI heating cases, which was obtained by the pinhole camera model using the database. It shows that the trajectories of the ablation cloud are bent to the toroidal direction of the NBI heating. The reason for the bending of the trajectories is possibly a jet effect by an asymmetric ablation process of the pellets caused by high energy ions produced by the NBI heating. When the interference filter was used, the visible emission of LiI($\lambda=671nm$) was observed in the last two or three frames of the ablation images. The positions of the LiI emission are also indicated in the figure, showing that the doped impurity (Li) was locally ablated in the plasma within about 3cm. The stereoscopic analysis of the ablation clouds clarified the three-dimensional trajectories of the ablation clouds and proved local deposition of the doped impurity in the plasmas by TESPEL injection.

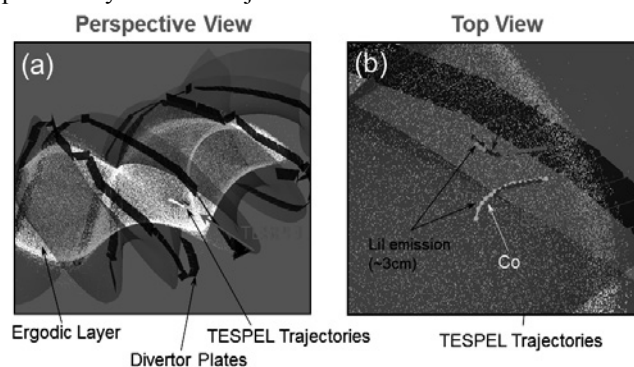


Fig. 2 (a) A perspective view of the three-dimensional trajectories of the TESPEL ablation clouds in the three different NBI heating cases, (b) an enlarged top view of the trajectories of the ablation clouds with showing the observed position of the LiI emission.

- 1) Tamura, N. et al.: Rev. Sci. Instr. **79**, No. 10 (2008) 10F541-1.
- 2) Sakamoto, R. et al.: Rev. Sci. Instr. **76**, No. 10 (2005) 103502.